ELSEVIER

Contents lists available at ScienceDirect

Journal of Colloid And Interface Science

journal homepage: www.elsevier.com/locate/jcis



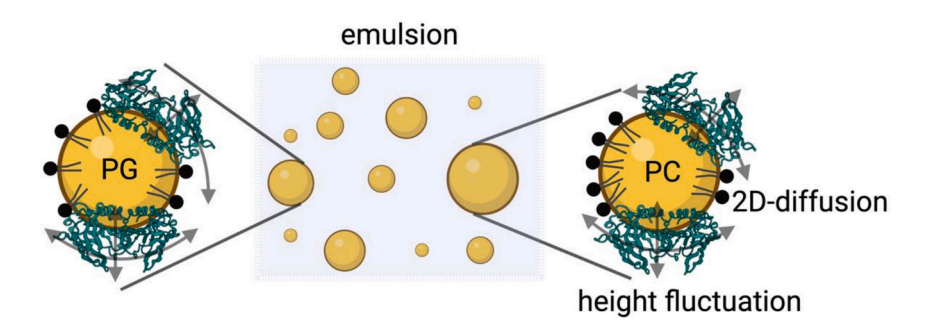


Phospholipids disrupt the interfacial network of proteins at the oil/water interface

Theresia Heiden-Hecht ^{a,*}, Maren Müller ^a, Sylvain Prevost ^b, Orsolya Czakkel ^b, Piotr Zolnierczuk ^c, Kuno Schwärzer ^d, Stephan Förster ^{a,d}, Henrich Frielinghaus ^a, Olaf Holderer ^a

- a Jülich Centre for Neutron Science (JCNS) at Heinz Maier-Leibnitz-Zentrum (MLZ), Forschungszentrum Jülich GmbH, Lichtenbergstr. 1, 85747 Garching, Germany
- ^b Institut Laue-Langevin, 71, avenue des Martyrs, 38042 Grenoble, France
- ^c Oak Ridge National Laboratory, P.O. Box 2008 MS 6460, Oak Ridge, TN 37831-6460, USA
- ^d Jülich Centre for Neutron Science (JCNS-1), Forschungszentrum Jülich GmbH, 52425 Jülich, Germany

GRAPHICAL ABSTRACT



ARTICLE INFO

Keywords: Oil/water interfaces Scattering Phospholipids B-Lactoglobulin Emulsion

ABSTRACT

Emulsions are part of everyday life, used, for example, in cosmetics, drug delivery, and food systems. Mixed interfaces in emulsions are quite common, and are composed of proteins and low molecular weight emulsifiers like phospholipids. However, research questions about the interfacial structure of mixed interfaces, such as their composition and arrangement, as well as their interfacial rheology and dynamics, remain unanswered.

In this study, we hypothesize that the charge and nature of phospholipid head groups have a strong impact on the interfacial structure and rheology of protein-stabilized emulsions, but barely influence their interfacial dynamics.

A combination of conventional methods – such as drop tensiometry and interfacial rheology – and advanced methods – such as small angle neutron scattering and neutron spin echo spectroscopy – helps us to answer research questions about complex interfacial systems.

The head group of phospholipids strongly affects the interfacial structure and rheology of a β -lactoglobulinstabilized emulsion. The interfacial structure was resolved using small-angle neutron scattering with partial structure factor analysis and coarse-grained modeling. The elastic interfacial protein layer is damaged by the addition of phospholipids. Phosphatidylcholine is loosely bound to the interface alongside β -lactoglobulin

E-mail address: t.heiden-hecht@fz-juelich.de (T. Heiden-Hecht).

 $^{^{\}star}$ Corresponding author.

molecules, whereas phosphatidylglycerol is partially bound to β -lactoglobulin molecules via hydrogen bonds or hydrophobic interactions. The interfacial dynamics are characterized by 2D diffusion within the interfacial layer of the oil droplet and height fluctuations normal to the interfacial layer. The interfacial dynamics of the protein are inert for changes in interfacial structure, composition, and rheology, although structure and rheology have a strong influence on each other. These results provide guidance for the emulsion characteristics of food, cosmetics, and drug delivery systems.

1. Introduction

Oil/water interfaces are ubiquitous in our day-to-day life. They can be found in cosmetics [1], drug delivery [2], and food systems [3]. These emulsion systems have been the focus of scientific research for the last few decades, addressing increasingly detailed research questions – from oscillating droplets [4] and the effect of crystallization behavior on oil droplet shape [5] to the processing of emulsions [6]. In cosmetics, drug delivery, and food, interfaces are often stabilized by proteins and/or low molecular weight emulsifiers such as phospholipids [1,2,7]. Mixed interfaces with proteins and low molecular weight emulsifiers combine the viscoelasticity of the protein at the interface with the fast interface stabilization and high interfacial activity provided by low-molecular-weight emulsifiers [8]. However, the mechanisms and interrelations between interfacial structure (e.g. composition and arrangement) and interface dynamics remain poorly understood. Conventional methods struggle to answer research questions about these aspects.

Our approach therefore combined *conventional methods* – such as static light scattering for oil droplet size, drop tensiometry for interfacial tension, dilatational rheology for interfacial elasticity, and interfacial shear rheology for interfacial network formation – with *advanced methods*, such as small-angle neutron scattering (SANS) for the structure of interfacial composition and arrangement, and neutron spin echo spectroscopy (NSE) for interfacial dynamics.

The objective of this study is to link the microscopic structure of the interface, as determined by small-angle scattering [9], with the macroscopic structure of the oil droplets within the emulsion via static light scattering. We also aim to link the microscopic elasticity, as obtained by neutron spin echo, with macroscopic elasticity and network formation determined by dilatational and interfacial shear rheology [10]. We hypothesize that the charge and nature of the head group of phospholipids has a strong impact on interfacial structure and rheology, but barely influences the dynamics of a mixed interface with β -lactoglobulin.

The experiments were performed with the main component of whey proteins (β -lactoglobulin), which is known for its high interfacial viscoelasticity and low interfacial tensions [10–12], together with common phospholipids (phosphatidylcholine and phosphatidylglycerol with unsaturated fatty acids), which are known for their strong interfacial activity in oil phases with saturated fatty acids [13–15]. Contrast variation is an important tool for the advanced methods, whereby we use either the deuterated or protonated form of a substance. Varying the contrast shifts the focus to different parts of the sample: the entire sample, the interfacial layer, the oil droplet, and the interfacial layer with the oil droplet. The combination of advanced and conventional methods allows us to answer many research questions about interfacial structure, rheology, and dynamics, which provide guidance for the emulsion characteristics of food, cosmetics, and drug delivery systems.

2. Experimental section

2.1. Materials

The emulsions and interfacial investigations were performed using β -lactoglobulin (β -lg) (Sigma Aldrich Chemie GmbH, Steinheim, Germany; purity of 99.5 %), phosphatidylcholine and phosphatidylglycerol with C18:1 fatty acids (Lipoid GmbH, Germany; purity 99.8 % and 98.8 %, respectively), and either protonated (WITARIX® MCT 60/40, IOI Oleo

GmbH, Hamburg, Germany) or synthesized deuterated MCT oil (method description in [16], purity >99 %, deuteration degree >91 %). The phospholipids were synthesized DOPC and DOPG-Na. Both lipids contained less than 0.05 % free fatty acids, had a peroxide number of 0, and contained less than 0.1 % lysophosphatidylcholine or lysophosphatidylglycerol. We opted for these phospholipids due to their difference in charge at pH 7 as well as their difference in organization (lamellar and micellar). The protonated (hMCT) and deuterated medium chain triacylglyceride oil (dMCT) were composed of C8 and C10 fatty chains with a ratio of 60 to 40. The density of the MCT oil was 0.945 g/cm^3 . Interfacial active substances in the protonated MCT oil were removed via magnesium silicate adsorption (Florisil®, Carl Roth GmbH, Karlsruhe Germany). The emulsions were prepared using an Ultra-Turrax device (IKA Werke, Staufen, Germany) at 25,000 rpm for 4 min with the addition of 5 w/w% MCT oil. Oil droplet size was captured multiple times in triplicate by means of static light scattering (LA-960 V2, Horiba *GmbH*, Kyoto, Japan) with $n_{oil} = 1.45$ and $n_{water} = 1.33$ for each sample preparation.

All interfacially active components were classified in their critical micelle concentration (CMC) or critical interfacial concentration (CIC) [11,14,15,17]. The CMC of phosphatidylcholine (PC) and phosphatidylglycerol (PG) was measured at 0.004 w/w% and 0.0045 w/w%, respectively, using drop tensiometry in triplicate at 20 °C and at pH 7 (method 2.2.1, see Fig. S7). PC reached an interfacial tension of 4 mN/m and PG a value of 15 mN/m above the CMC. PC formed micellar structures, while PG exhibited lamellar structures (see Fig. S8). The CIC of β -lg ranges between 0.1 w/w% and 0.3 w/w% [11], and was thus found to provide exact coverage of the interface for classical interfacial and emulsification methods [9,11]. In addition, the emulsions were classified by oil droplet size distribution. For β -lg-stabilized emulsions containing 0.25 w/w% protein, the oil droplet size ranged from 2.12 \pm 0.06 μm at the 10th percentile (D10) to 3.65 \pm 0.18 μm as the median (D50), and up to 6.20 \pm 0.71 μm at the 90th percentile (D90). The addition of 0.05 w/w% PC or 0.05 w/w% PG resulted in a comparable oil droplet size distribution with 2.18 \pm 0.09 μm at D10, 3.68 \pm 0.20 μm at D50, and up to 6.87 \pm 0.91 μm at D90 (PC), as well as 2.17 \pm 0.18 μm at D10, 3.72 \pm 0.26 μm at D50, and 6.81 \pm 0.65 μm at D90 (PG). Detailed data are shown in Table S2.

2.2. Preparation of β -lg solutions and MCT-oil phospholipid mixtures

The $\beta\text{-lg}$ solutions were prepared either in distilled H_2O or D_2O . The pH and pD were adjusted to 7 using 0.1 M NaOH and HCl or NaOD and DCl. The pH adjustment was recorded for at least 3 h under stirring conditions and then stored overnight at 5 $^{\circ}\text{C}$. The pH was then remeasured the following morning.

A 1w/w% stock solution of a phospholipid–MCT oil mixture was prepared for each measurement. The stock solution solubilized either phosphatidylcholine (PC) or phosphatidylglycerol (PG) under stirring conditions and a mild heat treatment of max. 50 °C. The dilution of the stock solution was performed either in protonated or deuterated form. The concentrations of β -lg and phospholipids were chosen to ensure either (i) a comparable oil droplet size distribution (0.25 w/w% β -lg and 0.05 w/w% PC or PG), or (ii) for drop tensiometry measurements, a stable droplet for the entire measurement time without droplet rupture due to low interfacial tension (0.01w/w% β -lg and 0.00001w/w% PC or PG). These concentrations were applied for all emulsion or interfacial

measurements.

2.3. Conventional methods for characterizing oil/water interfaces

2.3.1. Interfacial tension

The interfacial tension of the mixed interfaces stabilized with $\beta\text{-lg}$ and phospholipids was measured using a drop tensiometer OCA 15 EC (DataPhysics Instruments GmbH, Filderstadt, Germany). A droplet of a 0.01 w/w% $\beta\text{-lg}$ solution was generated in a cuvette of MCT oil with or without the partial addition of phosphatidylcholine or phosphatidylglycerol.

The measurements were performed at 20 °C.

2.3.2. Interfacial viscoelasticity

The interfacial viscoelasticity of the mixed interfaces was characterized by dilatational rheology and interfacial network formation. In both cases, the interface was ripened for 16 h before measuring the interfacial viscoelasticity in triplicate. For dilatational rheology, the interfacial film was stressed at 0.01 Hz with an amplitude of 3–19 % amplitude relative to the droplet area using an OCA 15 EC (DataPhysics Instruments GmbH, Filderstadt, Germany). For the interfacial network formation, the development of the interfacial layer was recorded for 16 h at 1 Hz and an amplitude of 0.1 % using a MCR102 rheometer (Anton Paar GmbH, Ostfildern, Germany). Further details of the methods are provided in the literature [10]. The measurements were performed at 20 °C.

2.3.3. Statistical analysis

Significance was evaluated using analysis of variance (ANOVA) to assess the differences in interfacial tension and interfacial network formation. Prior to analysis, data were tested for normal distribution using the Shapiro–Wilk test and for homogeneity using the Levene test. A two-way ANOVA and a post-hoc Tukey HS test were performed with a significance value of p < 0.05 using SPSS (Version 30, IBM, Armonk, New York).

2.4. Advanced methods characterizing interfaces within emulsions

2.4.1. Interface structure via small-angle neutron scattering

Small-angle neutron scattering (SANS) experiments were carried out using the D22 instrument at Institut Laue-Langevin, Grenoble, France. A collimated neutron beam hit the sample, with the neutrons scattered at low scattering angles being recorded. The scattering intensity was analyzed as a function of the scattering angle, or more commonly as a function of the modulus of the scattering vector:

$Q=4\pi/\lambda\,sin(\Theta/2)$

where λ is the neutron wavelength, Θ is the scattering angle, and Q relates to real-space length scales (d $=2\pi/Q$). Details on the technique can be found in the literature [18]. We used a collimation distance of 17.6 m with different detector distances: 17.6 m and 1.4 m. The neutron wavelength was set to 6 Å with a spread of ± 10 % (FWHM). The sample thicknesses were 1 mm and 2 mm. The latter thickness was only used when heavy water (approx. 95 % of the material) was used. All measurements were conducted at room temperature (22 °C) and within 24 h after emulsification. The measurements were corrected for the background of the empty cell, solvent scattering, and detector efficiency. Calibration was performed using 1 mm water as a secondary standard, accounting for transmission (measured separately) and sample thickness. All data were radially averaged, as the scattering was isotropic. The raw data can be found here: doi: https://doi.org/10.5291/ILL-DATA.9 -12-684.

In neutron scattering, the contrast between different components of the sample can be varied by appropriate isotope labeling, particularly by exchanging hydrogen (H) with deuterium (D) in part of the molecules in the sample. Table S1 in the supplementary information shows different scattering length densities (SLDs) of the components in the present sample. The most relevant situation for the present case is the use of heavy water (D₂O) with otherwise protonated components, especially "normal" MCT oil. The observation range in reciprocal space (Q $> 10^{-3}$ Å $^{-1}$) does not cover the full emulsion droplet size, which is measured using a particle sizer with static light scattering (see Table S2 in the Supplementary Information). Instead, it focuses on the interface between the oil droplet surface, decorated with proteins and lipids, and the water solvent (QR $_{\rm oildroplet}>>1$ in this area). In the case of deuterated oil (dMCT, see [16]) and D₂O, the main SLD difference arises from the interfacial layer alone relative to its surrounding (oil and water). Since the scattering intensity is measured in absolute units, the ratio of intensities can be used to infer the surface coverage of the oil droplet [9].

At larger Q values (>3 \times 10⁻² Å ⁻¹, i.e. molecular length scales), scattering from proteins and possibly from lipids play a role. Further details of the analysis are described in the "Results and discussion" and "Supplementary Information" sections.

2.4.2. Interface dynamics via neutron spin echo spectroscopy

The interface fluctuations were measured by neutron spin echo (NSE) spectroscopy using the SNS-NSE spectrometer operated by the Oak Ridge National Laboratory (Oak Ridge, USA) [19] at the Spallation Neutron Source (SNS) facility as well as the IN15 spectrometer (Institut Laue-Langevin, Grenoble, France) [20]. NSE provides the energy resolution required to measure thermally driven fluctuations. Similar to dynamic light scattering, NSE operates in the time domain and measures the normalized intermediate scattering function: I(Q,t) = S(Q,t)/S(Q,t)0) [21]. This is the Fourier transform of the time correlation function (or van Hove correlation function) from real space to reciprocal space. In contrast, dynamic light scattering measures correlation functions on very small scattering vectors, Q, (due to the long wavelength compared to neutrons) and on much longer time scales. NSE accesses molecular length scales and time scales up to several 100 ns, which correspond to the diffusive and thermally driven motion of larger molecules such as proteins. In addition, the contrast adaption capabilities of neutron scattering allow us to focus on particular parts of the sample, for example the proteins stabilizing the oil droplets in emulsions. A wavelength band of 5-8 Å was used at SNS-NSE, enabling Fourier times to reach about 40 ns with sufficient intensity. With the pulsed operation of the SNS, the data reduction from detector images to I(Q,t) allows for some flexibility in choosing the desired number of scattering vectors, Q, and Fourier time bins, t. For acceptable statistics within each bin, a Q resolution with 9 Q values and 15 t bins was chosen. Raw data reduction was performed with the NSE instrument software DrSPINE [22]. At IN15, two wavelength settings ($\lambda = 8$ and 13.5 Å) were used with four Q settings, allowing for a maximum Fourier time of 500 ns. The measurements were performed at 20 °C within 24 h after emulsification.

In this study, experimental data for all samples were first fitted with a stretched exponential function: $I(Q,t) = \exp(-(\Gamma t)^{\beta})$ where Γ is the relaxation rate. This allows us to investigate basic properties of the dynamics, such as the Q dependence of the relaxation and the stretching exponent β. For diffusive behavior, the relaxation rate exhibits a characteristic quadratic Q-dependence: $\Gamma = DQ^2$ where the Stokes–Einstein diffusion constant, D, is the proportionality factor, and $\beta = 1$. This applies, for example, to proteins in solution in our investigation. At length scales comparable to the diffusing objects, additional contributions from rotational motion or from internal dynamics, such as fluctuates between domains, are possibly accessible (for non-spherical objects). A fluctuating membrane sheet, such as the oil droplet interface, is well described by a Q^3 dependence of the relaxation rate, Γ , as formulated by Zilman and Granek [23], and also by a modification of the relaxation to a stretched exponential behavior with $\beta = 2/3$. Proteins at the oil droplet interface exhibit diffusive behavior with constraints imposed by the interface. The first analysis of the intermediate scattering function from NSE is therefore the Q dependence of the relaxation rate (e.g. $\Gamma/Q^2 = D$)

and the stretching behavior of the relaxation.

The interpretation of the relaxation rate and the resulting diffusion coefficients observed, D, can then include different contributions – from global large-scale diffusion of whole droplets (translational and rotational) and interface fluctuations to local motion of the proteins at the interface. Details of the analysis presented here can be found in section 3.3 together with the experimental data. The raw data can be found here: doi: https://doi.org/10.5291/ILL-DATA. 9-13-1127.

3. Results and discussion

3.1. Structure of interfaces within emulsions

The interfaces within the emulsions were first characterized using the advanced method SANS. The most important SANS spectra measured for bulk, film, and one intermediate contrast are shown in Fig. 1. The *bulk contrast* was obtained using protonated MCT oil (hMCT), protonated protein and phospholipid, and heavy water (D₂O), providing a contrast between the oil droplet and the surrounding D₂O. The *interfacial film contrast* was obtained using deuterated MCT oil (dMCT), protonated protein and phospholipid, and D₂O, where the surface layer on the oil droplet surface, consisting of proteins and lipids with a relatively low SLD, is surrounded by dMCT and D₂O with similar but higher SLDs. One *intermediate contrast* was obtained with dMCT, protonated protein and phospholipid, and a 60/40 H₂O/D₂O mixture, where the water mixture roughly corresponds to the SLD of the protein. Below, we also discuss other water mixing ratios that aim for zero contrast to either the protein or the phospholipid, since their natural contrasts differ.

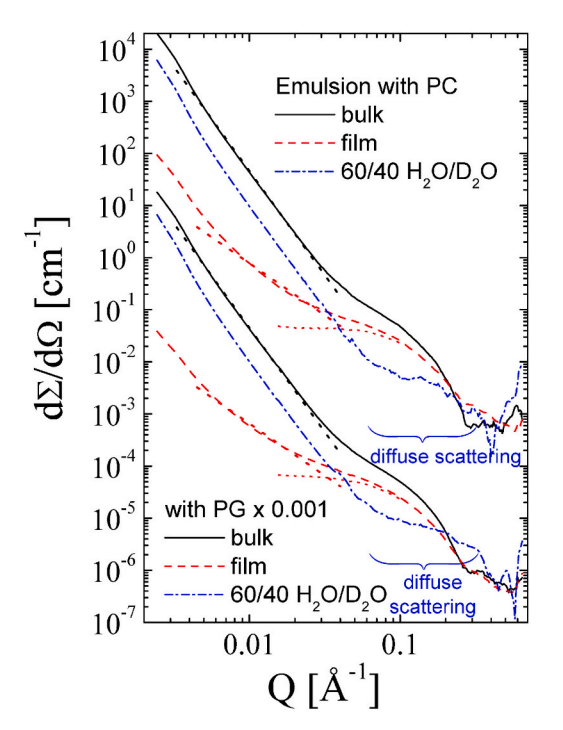
A striking difference between the measurements with and without lipid appears for the intermediate contrast (60/40 $\rm H_2O/D_2O)$, where strong diffuse scattering is observed between 0.007 $\rm \mathring{A}^{-1}$ and 0.3 $\rm \mathring{A}^{-1}$. The scattering intensity is about ten times higher than for the measurement without lipid where the statistical noise level is reached. In the

decomposition (see Supplementary Information), the different contributions of the scattering patterns clearly show almost constant diffuse scattering of the lipid and the protein. We attribute this to the loss of order in the protein network formed without lipid. The correlations of the proteins would appear as weak peaks below 0.007 $\rm \mathring{A}^{-1}$, but the strong power-law scattering dominates, and so this particular information is lost in our experiments.

In our previous paper, we derived formulae that connect different power laws to the amount of material in the film or interface consisting of protein and phospholipid [26]. The $Porod\ Q^{-4}$ power law describes the sharp interface of the oil droplet in relation to the residual components, while the film or interface Q^{-2} scattering describes a well-defined interface between the oil and water. Both power laws are indicated in Fig. 1 by dotted lines. When employing different power laws, we have to include the polydispersity corrections C_{Prorod} and $C_{interface}$. The main contributions arise from differences in contrasts (scattering length density differences $\Delta \rho$, see Table S1 in the Supplementary Information), interface coverage fractions, φ , and thicknesses of the considered interface, d (Table 1). We can thus obtain the intensity ratio for the Porod and interface scattering (see ref. [9]):

Table 1The interface coverages of different components obtained from the power laws of the SANS experiments.

Parameter	Without phospholipid	With PC	With PG
φ _{protein} (eq. 1)	80.3 %	72.0 %	73.6 %
φ _{total} (eq. 1)	_	104.0 %	84.4 %
$\phi_{lipid} = \phi_{total}$ - $\phi_{protein}$	_	32 %	11 %
φ _{lipid} (eq. 2)	_	27.7 %	14.8 %
d _{protein} [Å]	27	27	27
d _{lipid} [Å]	_	20	18



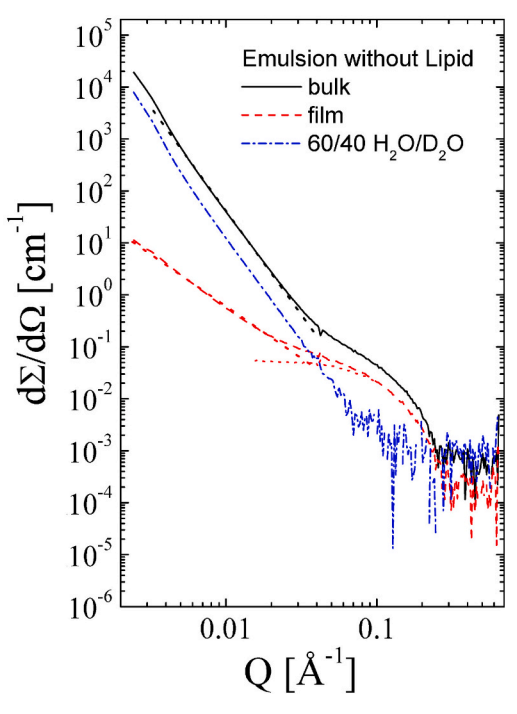


Fig. 1. The most relevant scattering contrasts of the SANS experiment on the emulsions with β -lg protein and the two phospholipids, PC and PG. The bulk contrast is obtained from hMCT, protonated protein and phospholipid, and D_2O . The interfacial film contrast is obtained from dMCT, protonated protein and phospholipid, and D_2O . The intermediate contrast is obtained from dMCT, protonated protein and phospholipid, and a $60/40~H_2O/D_2O$ mixture. The power-law scattering is indicated by the dotted straight lines. Guinier scattering from structure factor-free protein is indicated by the dotted red line for $Q > 0.01~\text{Å}^{-1}$. The incoherent background was always subtracted. (For interpretation of the references to colour in this figure legend, the reader is referred to the web version of this article.)

B: The most relevant scattering contrasts of the SANS experiment on the emulsions with β -lg protein without any phospholipid. The colors and lines are identical to Fig. 1A.

$$\frac{I_{\rm interface}}{I_{\rm Porod}}Q^{-2} = \left(\frac{\Delta\rho_{\rm interface}}{\Delta\varrho_{\rm Porod}}\right)^2 \bullet \varphi_{\rm interface} \bullet d_{\rm interface}^2 \bullet \frac{C_{\rm interface}}{C_{\rm Porod}}$$
(1)

The interface coverage fractions obtained in this way are summarized in Table 1 (lines 1–4) using eq. 1 with contrasts from Table S1, the thicknesses from Table 1, and the polydispersity corrections from static light scattering (Table S2). First, we identify the protein interface coverage as 72–74 % when phospholipid is added, and 80 % without the addition of phospholipid. The total interface coverage with phospholipid ranges from 84 % to 104 %. The value larger than 100 % reflects an uncertainty in the range of ± 4 %, which can be attributed to the statistical noise in the scattering experiment as well as additional uncertainties in the sample preparation. From the difference of the interface coverage, we can deduct the phospholipid interface coverage alone. With the phospholipid PC, the coverage is 32 %, while with PG, it amounts to 11 % – a considerable difference. While PC fills in all gaps of the interface, PG leaves significant open spaces between the protein molecules.

An alternative way of determining the interface coverage of the phospholipid alone is based on the relation between the interface coverage of the sample without phospholipid ($I_{\rm interface}$) and the complete coverage with phospholipid ($I_{\rm interface+lipid}$). Two identical power laws are then used, and polydispersity no longer plays an important role:

$$\frac{I_{\rm interface}}{I_{\rm interface+lipid}-I_{\rm interface}} = \left(\frac{\Delta \rho_{\rm protein}}{\Delta \varrho_{\rm lipid}}\right)^2 \bullet \frac{\varphi_{\rm protein}}{\varphi_{\rm lipid}} \bullet \left(\frac{d_{\rm protein}}{d_{\rm lipid}}\right)^2 \tag{2}$$

We can thus directly obtain the phospholipid interface coverage, which is in the range of 15 % to 28 %. The previously mentioned uncertainty of ± 4 % accounts for the differences with the other method described above. In all cases, PC fills all gaps at the interface between the proteins, while PG does not.

To obtain the protein scattering at $Q > 0.03 \text{ Å}^{-1}$, we used the *inter*facial film contrast scattering (Fig. 1) instead of the deconvoluted scattering function, S_{PP} , from the Supplementary Information due the large statistical noise here. We fitted a possible structure factor that also appears due to the film scattering, and divided the scattering data by this structure factor in order to obtain a flat Guinier scattering. We then fed this scattering function into the DENFERT program to obtain the pair correlation function, p(r), in real space and a reconstructed real-space structure (Fig. 2). In principle, the used contrast of the whole interface would also include the phospholipid structure as well. However, we obtained a pure dimer structure for the phospholipid PC. The space between different proteins therefore fluctuates and does not allow for the reconstruction of a real-space image of the surrounding phospholipid. For the phospholipid PG, a reconstructed phospholipid structure appears along the protein axis, while perpendicular to the axis it must be strongly fluctuating. The binding of the PG phospholipid must therefore be rather strong along the dimer axis.

3.2. Properties of oil/water interfaces

The oil/water interface was further characterized using conventional methods: drop tensiometry for interfacial tension, dilatational rheology for interfacial elasticity, and interfacial shear rheology for interfacial network formation.

The interfacial tension for β -lg was reduced to 16.6 mN/m over a period of 16 h. The addition of PG did not significantly change the interfacial tension (16.8 mN/m), while the addition of PC increased the interfacial tension to a value of 17.6 mN/m (see Table 2). Our measurements for β -lg are comparable to 0.1 % β -lg after 12 h of droplet ripening (15.8 mN/m) [12].

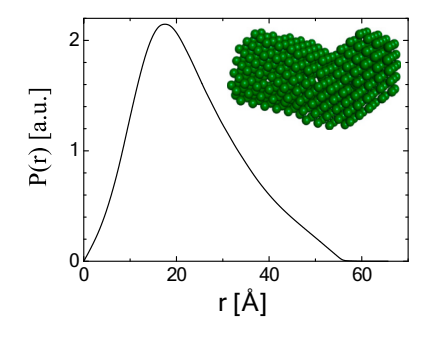
The interfacial network of β -lg was strong, with an elastic modulus G' of 22.5 mN/m and a viscous modulus G' of 4.4 mN/m. This interfacial network was disrupted by the addition of PC and PG, and led to low elastic moduli around 0 mN/m (see Table 2). Comparable data were reported for 0.1 % β -lg with 23 h of interfacial ripening (15 mN/m for G' and 3 mN/m for G'') [10].

For both interfacial tension and network, the differences between the $\beta\text{-lg}$ solution and the samples with PC and PG can be explained by the results from the interfacial structure within the emulsion. The addition of PC and PG disrupts the interfacial network. In the case of PG, PG binds to the protein and less phospholipid is adsorbed at the interface (Table 1 and Fig. 1). The interfacial layer loses elastic properties and the PG does not reduce the interfacial tension further. In the case of PC, it adsorbs loosely to the protein interfacial layer with a higher concentration than PG (Table 1 and Fig. 1). The interfacial layer loses elastic properties, but the interfacial tension also increases. Such an increase in interfacial tension is rather unusual. However, we also tested the addition of PC to the $\beta\text{-lg}$ solution with a concentration of 0.0001 %. Here, the droplet ruptured within a short time frame. Moreover, PC exhibited higher interfacial activity than PG during CIC measurements, as indicated in 2.1

For interfacial viscoelasticity, the data behave differently. The elastic modulus E' (Fig. 3) for β -lg started at a high level of 46 mN/m, and decreased with increasing amplitude to 20 mN/m (at 19 % amplitude).

Table 2 Interfacial tension and viscoelasticity of the interfacial network with the elastic modulus, G', and the viscous modulus, G'', for 0.01w/w% β-lg, with the partial addition of 0.00001w/w% phosphatidylcholine (PC) or phosphatidylglycerol (PG) at pH 7 after 16 h of interfacial ripening. The different letters (A, a, α , and B, b, b) indicate significant differences between the samples p < 0.05.

	Interfacial tension (mN/m)	G' (mN/m)	G"(mN/m)
β-Lg	$16.61\pm0.02~\text{a}$	$22.52 \pm 2.11 \ a$	$4.43\pm0.16~\text{A}$
+PC	$17.59 \pm 0.04 \text{ b}$	$-1.66 \pm 2.29 \ b$	$1.42\pm0.42~B$
+PG	$16.80 \pm 0.07 \text{ a}$	$-1.84 \pm 1.44 \ b$	$1.32\pm0.39~\mathrm{B}$



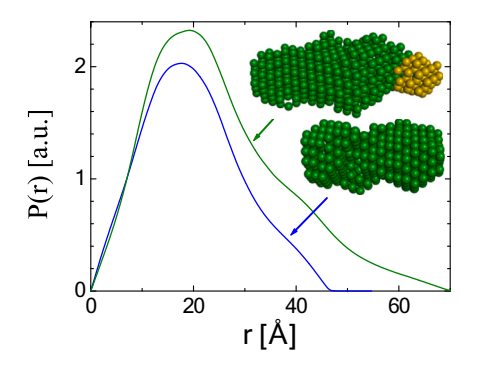


Fig. 2. The pair correlation function p(r) in real space, which mainly indicates the protein structure (left) for emulsions with the phospholipid PC (blue) and PG (green), and (right) for the emulsion without any phospholipid. The reconstructed real-space structures from the DENFERT program are also shown. The green spheres indicate the protein dimer and the yellow spheres depict the protein that is not fluctuating. (For interpretation of the references to colour in this figure legend, the reader is referred to the web version of this article.)

The elastic modulus for β -lg with the addition of PC or PG started at a lower level of 38 mN/m and 29 mN/m, respectively. Both β -lg phospholipid mixtures showed a reduction in the elastic modulus with increasing amplitude. The reduction in elasticity was more pronounced for β -lg and PG.

Since the addition of PC or PG damages the interfacial network, this also causes changes in the interfacial viscoelasticity. The elastic modulus of both samples with phospholipids is also reduced. Due to the loosely bound structure between $\beta\text{-lg}$ and PC (see Table 1 and Fig. 2), desorption and adsorption behavior during the oscillation of the droplet cause a lower reduction in the elastic modulus with increasing amplitude. This phenomenon is particularly pronounced for the high amplitudes.

3.3. Dynamics of interfaces within emulsions

The dynamics on a molecular scale were studied with NSE. In general, two types of dynamics may be considered for the protein-stabilized emulsion interface: (i) a (possibly constrained) 2D diffusion in the interface plane, and (ii) height fluctuations of the interface layer. In the following paragraphs, the possible contributions of the different types of dynamics are described.

2D diffusion on the droplet interface: The 2D diffusion of a cylinder in a membrane is described by the Saffman–Delbrück model. This model was developed for the motion of membrane proteins in a phospholipid bilayer [24]. If the interface viscosity in this model is simply the average of the oil and water viscosities, then the mean square displacement <u 2 > is related to the Stokes–Einstein diffusion coefficient by <u 2 \ge 4Dt, which is the result for translational diffusion on a two-dimensional plane. In the three-dimensional case, <u 2 \ge 6Dt, meaning that the interface mobility contributes to two-thirds of the overall displacement.

Additionally, *fluctuations perpendicular to the membrane* will also be present. The model of a fluctuating membrane patch by *Zilman and Granek* [23] describes interfacial height fluctuations, but in the case of a protein-stabilized interface, the SANS experiments showed that the signal is a mixture of the protein form factor and the interface contribution with the characteristic Q^{-2} decay at low Q (see Fig. 4 and Supplementary Information). Proteins will also follow the height fluctuations in the z-direction and therefore present dynamics that can be described by the Zilman–Granek model if this part can be described as a coherent interface fluctuation. If the proteins at the interface fluctuate individually in the z-direction, a 1D diffusive contribution will be

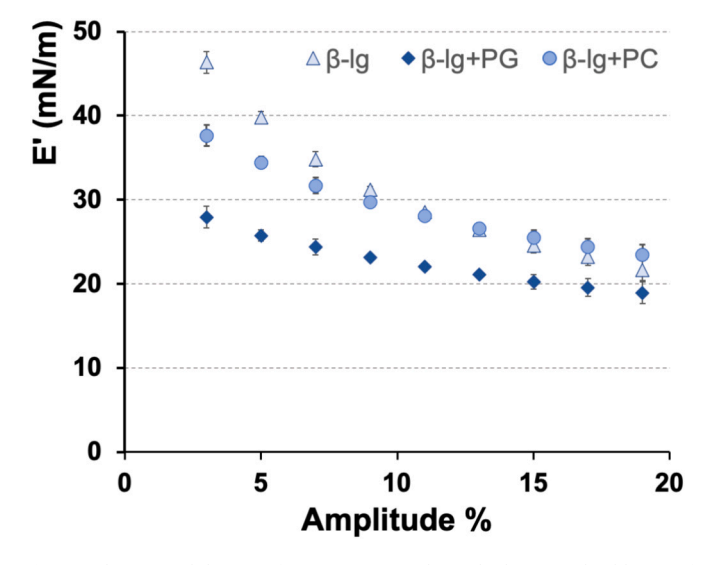


Fig. 3. Elastic modulus, E', for 0.01 w/w% β -lg with the partial addition of 0.00001 w/w% phosphatidylcholine (PC) or phosphatidylglycerol (PG) at pH 7 after 16 h of interfacial ripening, captured at 3–19 % amplitude in relation to the droplet area, at 0.01 Hz.

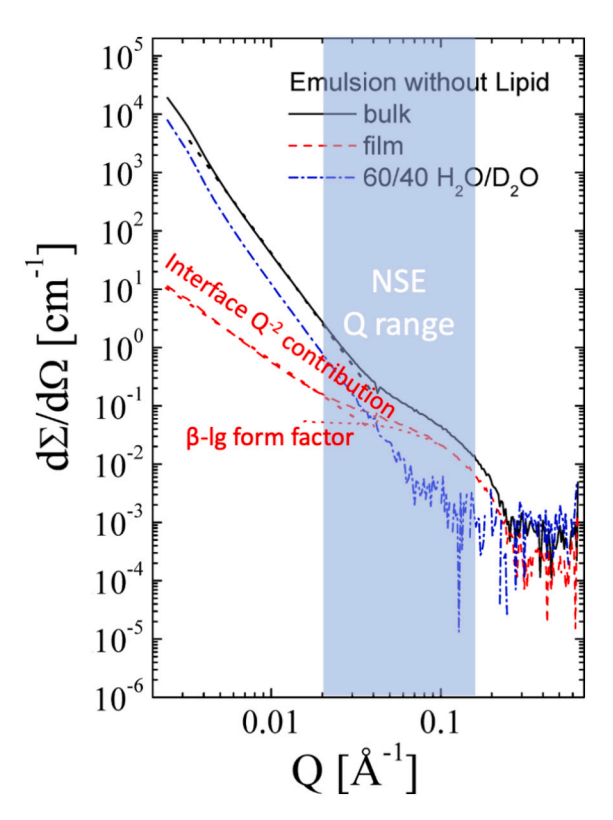


Fig. 4. Contributions to the dynamic structure factor comprise the interface scattering at low Q and the protein form factor. *NSE experiments were performed in film contrast* (D_2O , dMCT).

observed. The main difference between Zilman–Granek membrane fluctuations and 1D diffusion in the z-direction with constraints is the additional Q-dependence of the dynamics.

Since the interfacial layer is rather densely packed with proteins – as corroborated by SANS [9] – the 2D diffusion in the plane will also experience some "caging effects" from the surrounding proteins when $<\!u^2>$ approaches the length scale of the protein of the order of 8 nm (long axis for a β -lg dimer). This reduces the relaxation rate at longer length scales (or smaller Q in NSE). Moreover, the increasing contribution of the interface dynamics and the decreasing contribution of the protein motion become visible below $\sim\!0.08~\textrm{Å}^{-1}$, where the interface scattering emerges in the SANS intensity.

For this study, Fig. 5 shows the effective diffusion constant D_{eff} (i.e. $\Gamma/Q^2)$, which is obtained from a fit of the intermediate scattering function I(Q,t) measured with NSE (see Supplementary Information, Figs. S5, S6) using a stretched exponential function. This results in a relaxation rate Γ and a stretching exponent β . A correction for the stretching exponent β must be applied according to $D_{eff}=\beta\,\Gamma/Q^2/\gamma(1/\beta)$, in order to make D_{eff} comparable. Here, γ is the Gamma function – not to be confused with the relaxation rate, Γ , for the β -lg in solution and for the different emulsions – and $\beta\,\Gamma/\gamma(1/\beta)$ is the mean relaxation rate of the stretched exponential function.

For β -lg in solution, a Q^2 -dependence (i.e. a constant value of D_{eff}) is clearly observed, as expected for diffusive motion (see Fig. 5). The pure protein diffusion is $D_{eff}=7.3+/-0.1~\text{Å}^2/\text{ns}$. The Q-range for the protein solution was not extended to low Q, since for these rather dilute samples we do not expect structure factor influences, and D_{eff} at $Q\sim0.06~\text{Å}^{-1}$ already represents the long-range diffusion, as shown for a similar dimeric protein BSA [25]. All emulsions, stabilized either with pure protein or additionally with interfacially active phospholipids PG and PC had a slightly lower average diffusion coefficient in the Q-region with constant D_{eff} , where protein motion dominates: around 4.6–5.2 Å $^2/\text{ns}$ (emulsion: 5.2 +/- 0.2, PC emulsion: 4.9 +/- 0.1, PG emulsion 4.6

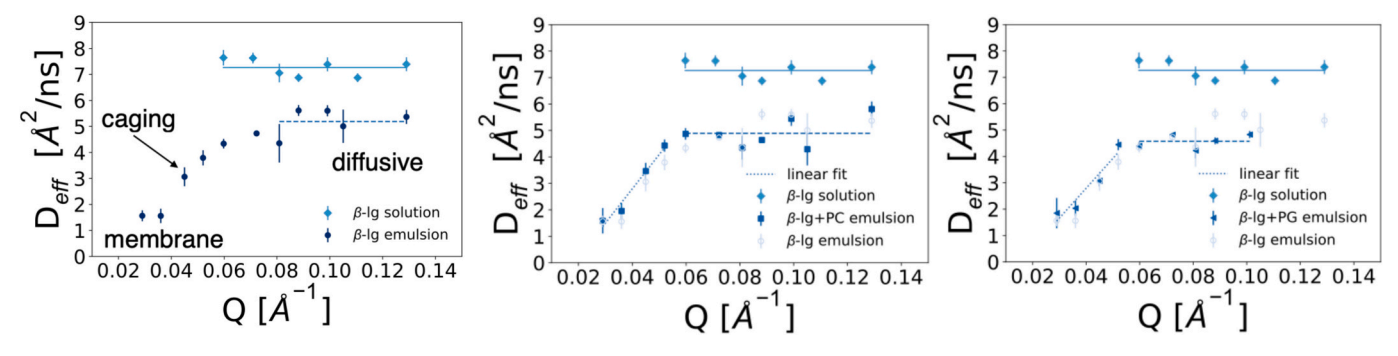


Fig. 5. Effective diffusion as a function of Q. Below $Q=0.08~\text{Å}^{-1}$, a linear increase is observed for the emulsions, while at a higher Q, D_{eff} is almost constant. The local protein motion (diffusive motion) at $Q>0.08~\text{Å}^{-1}$ is slightly reduced compared to the free three-dimensional diffusion of β-lg in solution (averaged D_{eff} from IN15 and SNS-NSE). A strong caging effect can be observed below $Q\sim0.08~\text{Å}^{-1}$, while at a very low Q, the scattering and the dynamics are dominated by the membrane fluctuation of the interface (Q^{-2} scattering from SANS).

+/- 0.1 Ų/ns). The contribution of a pure, unhindered 2D diffusion on the interface of the emulsion droplet would be two-thirds of the 3D value of D_{eff} (2/3 \times 7.3 =4.9 Ų/ns). The measured diffusion coefficient for all emulsions likely also includes an additional contribution of the height fluctuations, as will be discussed below. Due to the droplet size $>1~\mu m$, overall droplet translational or rotational diffusion does not contribute to the dynamics on the length- and time-scales of the NSE experiment.

With a diffusion constant for the protein in solution of D = $7.3\,\text{Å}^2/\text{ns}$, the corresponding length scale of the root mean squared displacement at a time of 40.0 ns is $<\text{u}^2>^{(1/2)}=(6\text{Dt})^{(1/2)}=4$ nm in 3D, while in 1D (only 'z' contribution) it is 1/3 RMSD = 1.4 nm, corresponding to the approximate distance which the protein moves perpendicular to the interface during this time interval.

The diffusion coefficient of the β -lg emulsions containing the phospholipids PC and PG are similar to that of the pure emulsion, with a slight decrease observable for the PG emulsion. The effect of the phospholipids on height fluctuations and on the in-plane mobility at molecular length scales will be discussed below in more detail.

In the emulsions studied here, we observe a deviation from the Q^2 behavior below $Q<0.08~\mbox{\normalfont\AA}^{-1}$ for the pure emulsion, indicated by a gradual change in slope. The emulsions containing PC and PG show this deviation from a constant D_{eff} below $Q<0.06~\mbox{\normalfont\AA}^{-1}$, corresponding to characteristic length scales of $2\pi/Q$ of about 8 nm for the pure emulsion and 10 nm for the emulsions with PC and PG.

The sudden decrease of D_{eff} at low Q by a factor of ${\sim}3$ cannot be attributed to the slightly larger interface scattering compared to the protein form factor contribution (see Supplementary Information). Instead, it clearly indicates jamming at the interface, as β -lg proteins are hindered from diffusing further on the oil droplet interface than the above-mentioned ${\sim}10$ nm distance. The change in D_{eff} therefore reflects a mixture of (predominantly) blocked 2D diffusion on the droplet interface and Q-dependent diffusion from height fluctuations according to Zilman and Granek, where $D_z(Q) \sim k_B T/(6\pi\eta)(k_B T/\kappa)^{1/2}~Q$ (see Supplementary Information).

The curve shape of the decay in S(Q,t) can indicate the nature of mobility – either membrane height fluctuations with a stretched exponential decay or diffusive behavior with a simple exponential decay. The stretching exponent β is 1~(+/-~0.1) for the pure protein in solution (individually fitted to each Q), as expected for particles following Stokes–Einstein diffusion, with a simple exponential decay of I(Q,t), as presented in Fig. S6. The emulsions are best fitted with a slightly lower β (0.9~+/-~0.1), which is typical for deviations from pure diffusive behavior. For pure membrane fluctuations, $\beta=2/3$ could be expected. The observed β is in good agreement with the mixture of protein scattering and interface scattering (see Supplementary Information). As described above, the deduced diffusion coefficient D_{eff} was corrected for the effects of different stretching exponents by using the *mean relaxation rate*, making the values comparable.

The Q^2 -dependence at large Q therefore indicates that the protein or protein/phospholipid layer does not form a fully continuous rigid interface, but still exhibits some reduced in-plane mobility on the length scales corresponding to the molecular size, along with a significant "jamming" effect on larger length scales. Hydrodynamic interactions, which influence the diffusion constant in concentrated solutions at low Q, may be seen as a related effect [26,27]. Above $Q=0.07~\text{Å}^{-1}$, this no longer plays a significant role, and only the combination of 2D diffusion and interface height fluctuations contribute to the dynamics.

An upper limit for the height fluctuation contribution is the lowest value of D_{eff} at low Q, which is 1.5 Å $^2/ns.$ According to $D_z(Q) \sim (k_BT/(6\pi h))(k_BT/\kappa)^{1/2} \;\; Q$ (Zilman–Granek model), this corresponds to a bending rigidity of about 18 $k_BT.$ This should be considered a lower limit for $\kappa,$ since long-range diffusive behavior of β -lg on the emulsion droplet interface towards very low Q cannot be definitively determined due to the accessible Q-range of the NSE.

The interfacial tension contribution resulting from a bending rigidity of $18~k_BT$ over a lateral distance of r=8.2~nm is 2.2~mN/m (with $2\kappa/r^2=\gamma_{bend}$), see also [28] and Supplementary Information. This value is lower than the total interfacial tension, meaning that κ contributes about 10--20~% to the interfacial tension.

The two phospholipids serve as lubricants between the proteins and break up the rather strong network between the protein dimers that interact through hydrogen bonds, as observed by interfacial rheology. It should be noted that the dimers are already highly crowded at the interface. While PC shows a tendency to fully cover the interface, and therefore has a higher extensional modulus similar to the purely proteincovered interface, PG leaves spaces uncovered and therefore has a lower extensional modulus. The higher-Q NSE data reveal 2D diffusion of the encaged protein dimers, which appear to be largely unaffected by networking or lubrication. The dimers are already highly crowded (as seen from the interface coverage) and the dominating modes of movement are therefore largely unaltered by the phospholipid. Interestingly, the caging observed at lower-Q NSE also appears to be very similar for all systems, and only the large-scale diffusion (which could not be resolved by NSE) might display differences. This topic therefore leaves open questions for future measurements and highly interesting details about the stabilization mechanisms in emulsions.

Expanding the accessible Q-range further towards even lower Q values and extending the time range towards μs might enable a better separation of bending modes from other diffusive modes at the interface. This will help us to better understand the stabilization mechanisms in emulsions.

4. Conclusions

The combined approach of advanced and conventional methods enables us to answer many research questions about the interfacial structure, rheology, and dynamics of any interface. These results provide insights for the characteristics of emulsions in food, cosmetics, and drug delivery systems. The interfacial structure affects the interfacial rheology, which in turn governs emulsion stability. A highly elastic interfacial layer stabilizes the emulsion against destabilization mechanisms. The interfacial dynamics affect emulsion destabilization processes such as coalescence.

In this study, we chose to investigate a complex mixed interface stabilized by β -lactoglobulin and phospholipids. We found that the head group of phospholipids strongly affects both interfacial structure and rheology. The interfacial structure was resolved through detailed data analysis of small-angle neutron scattering results. Contrast variation between oil, water, and interface components allowed us to obtain partial structure factors and thus gain an exceptionally detailed understanding of the structure of the multi-component interface. Assigning the results to specific scattering functions and cross-correlations, followed by coarse-grained modeling, enabled us to determine the interfacial composition and arrangement. Phosphatidylcholine is loosely bound to the interfacial layer alongside the β -lactoglobulin molecules. Phosphatidylglycerol is partly bound to the β -lactoglobulin molecule due to hydrophobic interactions or hydrogen bonds, but it is also partly loosely attached to the interfacial layer.

The β -lactoglobulin interface formed a viscoelastic interfacial layer with a strong elastic network. The addition of phospholipids disrupted this interfacial network. The rheology of the sample containing loosely bound phosphatidylcholine is dominated by desorption and adsorption behavior, particularly at high amplitudes.

Another study investigated the interfacial properties of β -lactoglobulin-stabilized emulsions with the addition of phosphatidylcholine or phosphatidylethanolamine containing either 18:0 or 18:1 fatty acids [29]. The unsaturated phospholipids displaced the proteins [29], as was partly observed in our study. Displacement effects at the interface are always dependent on the concentration ratio used.

Interfacial dynamics at the molecular level are described by 2D diffusion within the interfacial layer of the oil droplet, and by height fluctuations perpendicular to the interfacial layer. The diffusion coefficient of β -lactoglobulin in all interfacial layers of the emulsions is only slightly reduced compared to the free 3D protein diffusion in solution. The proteins remain mobile on molecular length scales. A strong jamming effect is observed for length scales that are roughly larger than the dimension of the β -lactoglobulin.

Local protein mobility appears to be an important property of this type of stable emulsion, which is present both with and without protein network formation at the interface. The challenges of NSE experiments on samples with a very low protein concentration and with limited stability meant that the accessible Q-range is limited. Extending this range to both smaller and larger Q values will be the aim of future studies. It can also help to provide further insights into the interfacial 2D mobility of "free", jammed, and 2D-cross-linked proteins at the interface, and how this relates to the rheological properties and macroscopic function of protein-stabilized emulsions.

CRediT authorship contribution statement

Theresia Heiden-Hecht: Writing – original draft, Visualization, Supervision, Methodology, Investigation, Formal analysis, Conceptualization. Maren Müller: Writing – review & editing, Investigation. Sylvain Prevost: Methodology, Investigation. Orsolya Czakkel: Methodology, Investigation. Piotr Zolnierczuk: Methodology, Investigation. Kuno Schwärzer: Methodology. Stephan Förster: Writing – review & editing, Supervision. Henrich Frielinghaus: Writing – review & editing, Visualization, Validation, Methodology, Investigation. Olaf Holderer: Writing – original draft, Visualization, Validation, Methodology, Investigation, Formal analysis.

Declaration of competing interest

The authors declare that they have no known competing financial interests or personal relationships that could have appeared to influence the work reported in this paper.

Acknowledgements

The authors are grateful for the help received during the synthesis of MCT oil, in particular the synthesis of fatty acids at the ISIS deuteration facility with special assistance from Yao Chen and Peixun Li, and the theoretical and methodical input from Jürgen Allgaier located at the deuteration lab of Forschungszentrum Jülich GmbH. Moreover, Alexandros Koutsioumpas helped with discussions on the coarse-grained modeling of protein structure/shape. We would also like to acknowledge the free sample supply provided by Lipoid GmbH and IOI-Oleo GmbH. Tom Brooks, as part of the Jülich language service, improved the language of this study.

Appendix A. Supplementary data

Supplementary data to this article can be found online at https://doi.org/10.1016/j.jcis.2025.139095.

Data availability

Data will be made available on request.

References

- [1] G. Secchi, Role of protein in cosmetics, Clin. Dermatol. 26 (2008) 321–325, https://doi.org/10.1016/j.clindermatol.2008.04.004.
- [2] M. Martins, A. Loureiro, N.G. Azoia, C. Silva, A. Cavaco-Paulo, Protein formulations for emulsions and solid-in-oil dispersions, Trends Biotechnol. 34 (2016) 496–505, https://doi.org/10.1016/j.tibtech.2016.03.001.
- [3] E. Dickinson, Emulsions, Annu. Rep. Prog. Chem., Sect. C: Phys Chem. 83 (1986) 31–58, https://doi.org/10.1039/PC9868300031.
- [4] A.S. Lodge, Oscillating droplets and spontaneous emulsification, Nature 4487 (1955) 839–840.
- [5] N. Denkov, S. Tcholakova, I. Lesov, D. Cholakova, S.K. Smoukov, Self-shaping of oil droplets via the formation of intermediate rotator phases upon cooling, Nature 528 (2015) 392–395, https://doi.org/10.1038/nature16189.
- [6] J. Atencia, D.J. Beebe, Controlled microfluidic interfaces, Nature 437 (2005) 648–655.
- [7] E. Dickinson, Mixed biopolymers at interfaces: competitive adsorption and multilayer structures, Food Hydrocoll. 25 (2011) 1966–1983, https://doi.org/ 10.1016/j.foodhyd.2010.12.001.
- [8] B.S. Murray, Interfacial rheology of food emulsifiers and proteins, Curr Opin colloid, Interface Sci. 7 (2002) 426–431, https://doi.org/10.1016/S1359-0294(02) 00077-8
- [9] T. Heiden-Hecht, B. Wu, K. Schwärzer, S. Förster, J. Kohlbrecher, O. Holderer, H. Frielinghaus, New insights into protein stabilized emulsions captured via neutron and X-ray scattering: an approach with β-lactoglobulin at triacylglycerideoil/water interfaces, J. Colloid Interface Sci. 655 (2024) 319–326, https://doi.org/ 10.1016/j.jcis.2023.10.155.
- [10] T. Heiden-Hecht, M. Ulbrich, S. Drusch, M. Brückner-Gühmann, Interfacial properties of β-lactoglobulin at the oil/water interface: influence of starch conversion products with varying dextrose equivalents, Food Biophys. 16 (2021) 169–180. https://doi.org/10.1007/s11483-020-09658-4.
- [11] H. Schestkowa, S. Drusch, A.M. Wagemans, FTIR analysis of β-lactoglobulin at the oil/water-interface, Food Chem. 302 (2020) 125349, https://doi.org/10.1016/j. foodchem.2019.125349.
- [12] J.K. Keppler, A. Heyse, E. Scheidler, M.J. Uttinger, L. Fitzner, U. Jandt, T.R. Heyn, V. Lautenbach, J.I. Loch, J. Lohr, H. Kieserling, G. Günther, E. Kempf, J.H. Grosch, K. Lewiński, D. Jahn, C. Lübbert, W. Peukert, U. Kulozik, S. Drusch, R. Krull, K. Schwarz, R. Biedendieck, Towards recombinantly produced milk proteins: physicochemical and emulsifying properties of engineered whey protein betalactoglobulin variants, Food Hydrocoll. 110 (2021) 106132, https://doi.org/10.1016/i.foodhyd.2020.106132.
- [13] T. Heiden-Hecht, S. Drusch, Impact of saturation of fatty acids of phosphatidylcholine and oil phase on properties of β-lactoglobulin at the oil/water interface, Food Biophys 17 (2021) 171–180, https://doi.org/10.1007/s11483-021-09705-8
- [14] E. Hildebrandt, A. Dessy, J.H. Sommerling, G. Guthausen, H. Nirschl, G. Leneweit, Interactions between phospholipids and organic phases: insights into lipoproteins and nanoemulsions, Langmuir 32 (2016) 5821–5829, https://doi.org/10.1021/ acs.langmuir.6b00978.

- [15] R. Pichot, R.L. Watson, I.T. Norton, Phospholipids at the interface: current trends and challenges, Int. J. Mol. Sci. 14 (2013) 11767–11794, https://doi.org/10.3390/ iims/40611752
- [16] K. Schwärzer, T. Heiden-Hecht, Y. Chen, O. Holderer, H. Frielinghaus, P. Li, J. Allgaier, Synthesis of deuterated and Protiated Triacylglycerides by using 1,1'-Carbonyldiimidazole activated fatty acids, Eur. J. Org. Chem. (2023), https://doi. org/10.1002/ejoc.202300632.
- [17] A. Zumbuehl, Artificial phospholipids and their vesicles, Langmuir 35 (2019) 10223–10232, https://doi.org/10.1021/acs.langmuir.8b02601.
- [18] C.J. Gommes, S. Jaksch, H. Frielinghaus, Small-angle scattering for beginners, J. Appl. Crystallogr. 54 (2021) 1832, https://doi.org/10.1107/ \$1600576721010223
- [19] M. Ohl, M. Monkenbusch, N. Arend, T. Kozielewski, G. Vehres, C. Tiemann, M. Butzek, H. Soltner, U. Giesen, R. Achten, H. Stelzer, B. Lindenau, A. Budwig, H. Kleines, M. Drochner, P. Kaemmerling, M. Wagener, R. Möller, E.B. Iverson, M. Sharp, D. Richter, The spin-echo spectrometer at the spallation neutron source (SNS), Nucl Instrum Methods Phys Res A 696 (2012) 85–99, https://doi.org/ 10.1016/j.nima.2012.08.059.
- [20] B. Farago, P. Falus, I. Hoffmann, M. Gradzielski, F. Thomas, C. Gomez, The IN15 upgrade, Neutron News 26 (3) (2015) 15–17, https://doi.org/10.1080/10448632.2015.1057052.
- [21] D. Richter, M. Monkenbusch, A. Arbe, J. Colmenero, Neutron Spin Echo in Polymer Systems, SpringerBerlin, Heidelberg, 2005.

- [22] P.A. Zolnierczuk, O. Holderer, S. Pasini, T. Kozielewski, L.R. Stingaciud, M. Monkenbusche, Efficient data extraction from neutron time-of-flight spin-echo raw data, J. Appl. Crystallogr. 52 (2019) 1022–1034, https://doi.org/10.1107/ S1600576719010847.
- [23] A.G. Zilman, R. Granek, Undulations and Dynamic Structure Factor of Membranes 77, 1996, pp. 4788–4791.
- [24] P.G. Saffman, M. Delbrock, Brownian motion in biological membranes (diffusion) 72, 1975, pp. 3111–3113. https://www.pnas.org.
- [25] F. Ameseder, R. Biehl, O. Holderer, D. Richter, A.M. Stadler, Localised contacts lead to nanosecond hinge motions in dimeric bovine serum albumin, Phys. Chem. Chem. Phys. 21 (2019) 18477–18485, https://doi.org/10.1039/c9cp01847f.
- [26] E. Buvalaia, M. Kruteva, I. Hoffmann, A. Radulescu, S. Förster, R. Biehl, Interchain hydrodynamic interaction and internal friction of polyelectrolytes, ACS Macro Lett. 12 (2023) 1218–1223, https://doi.org/10.1021/acsmacrolett.3c00409.
- [27] U.K.R. Genz, Collective Diffusion of Charged Spheres in the Presence of Hydrodynamic Interaction, Physica A: Statistical Mechanics and Its Applications, 1991, pp. 26–42.
- [28] E. Scholten, L.M.C. Sagis, E. Der Van Linden, Effect of bending rigidity and interfacial permeability on the dynamical behavior of water-in-water emulsions, J. Phys. Chem. B 110 (2006) 3250–3256, https://doi.org/10.1021/jp056528d.
- [29] K. Risse, J.L. Bridot, S. Bäther, L. Sagis, S. Drusch, Towards tailoring the viscoelasticity of liquid-liquid interfaces in emulsions: understanding phospholipid-protein interactions at the oil-water interface, Food Hydrocoll. 169 (2025), https://doi.org/10.1016/j.foodhyd.2025.111594.